Experimental Investigation of Energy Storage Properties and Thermal Conductivity of A Novel Organic Phase Change Material/MXene as A New Class of Nanocomposites

Navid Aslfattahi[1,*], R. Saidur[2, 4,*], A. Arifutzzaman[2], R. Sadri[3], Nuno Bimbo[4], Mohd Faizul Mohd Sabri[1,*], Philip A Maughan[4], Luc Bouscarrat[4], Richard J Dawson[4], Suhana Mohd Said[5], Boon Tong Goh[3] , Nor Azwadi Che Sidik[6]

[1] Department of Mechanical Engineering, Faculty of Engineering, University of Malaya, 50603, Kuala Lumpur
[2] Research Center for Nano-Materials and Energy Technology (RCNMET), School of Science and Technology, Sunway University, Bandar Sunway, Petaling Jaya, 47500, Selangor Darul Ehsan, Malaysia
[3] Low Dimensional Materials Research Centre, Department of Physics, Faculty of Science, University of Malaya, 50603, Kuala Lumpur, Malaysia
[4] Department of Engineering, Lancaster University, Lancaster, LA1 4YW, UK
[5] Department of Electrical Engineering, Faculty of Engineering, University of Malaya, 50603, Kuala Lumpur
[6] Malaysia – Japan International Institute of Technology (MJIIT), University Teknologi Malaysia, Jalan Sultan Yahya Petra,54100 Kuala Lumpur, Malaysia

Corresponding authors: Navid.fth87@yahoo.com, Saidur@sunway.edu.my, Faizul@um.edu.my

Abstract

Energy storage is a global critical issue and important area of research as most of the renewable sources of energy are intermittent. In this research work, recently emerged inorganic nanomaterial (MXene) is used for the first time with paraffin wax as a phase change material (PCM) to improve its thermo-physical properties. This paper focuses on preparation, characterization, thermal properties and thermal stability of new class of nanocomposites induced with MXene nanoparticles in three different concentrations. Acquired absorbance (UV-Vis) for nanocomposite with loading concentration of 0.3 wt.% of MXene achieved ~39% enhancement in comparison with the pure

paraffin wax. Thermal conductivity measurement for nanocomposites in a solid state is performed using a KD2 PRO decagon. The specific heat capacity (c_p) of PCM based MXene is improved by introducing MXene. The improvement of c_p is found to be 43% with 0.3 wt.% of MXene loaded in PCM. The highest thermal conductivity increment is found to be 16% at 0.3 wt.% concentration of MXene in PCM. Decomposition temperature of this new class of nanocomposite with 0.3 wt.% mass fraction is increased by ~6%. This improvement is beneficial in thermal energy storage and heat transfer applications.

Keywords. MXene, PCM, Thermal energy storage, Thermal conductivity, Thermal stability

1. Introduction

Using renewable energies is one of the solutions for many environmental challenges that we face today. Solar energy is regarded as the most prominent source of renewable energy moving forward as the hourly incident solar flux on the surface of the earth is more noteworthy than annual global energy consumption [1]. Solar thermal harvesting was studied extensively over the last decade and therefore it became one of the most efficient and reliable technologies for supplying energy. To make thermal energy storage (TES) cost effective and efficient, further improvement with the introduction of emerging nano-materials is needed. TES offered promising solutions to the world's energy as well as environmental challenges [2, 3]. An effective way to store thermal energy is employing a latent heat storage system with organic/inorganic phase change material (PCM). PCMs can absorb and/or release a remarkable amount of latent heat as a result of a phase transition when the phase transition temperature is within a specified temperature range. Phase change phenomenon (encapsulated PCM) is explained in Figure 1.

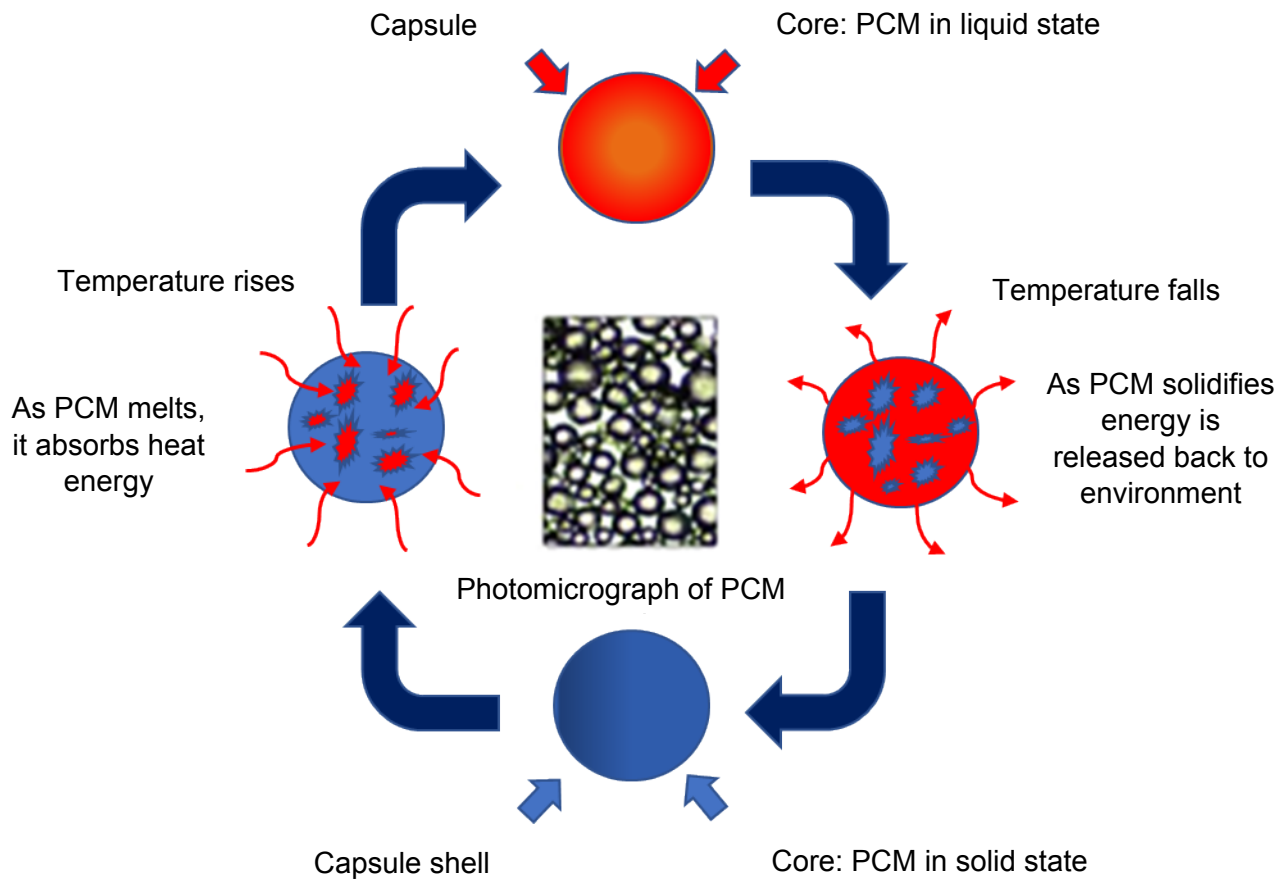

Figure 1. Performance of organic/inorganic phase change materials in solid/liquid states (encapsulated PCM) [4]

PCMs were applied in the area of both thermal isolation and energy storage, such as air-conditioning [5], solar thermal storage [6, 7], building energy management [8, 9]. Phase change temperatures and phase transition enthalpies are dependent on materials [10]. The choice of a correct PCM depends generally on proper thermal characteristics for a specific application, in addition to its stability and cost. PCMs are classified into organic, inorganic, and eutectics according to their chemical composition and structure. Their details are explained in [4, 11, 12]. Table 1 demonstrates a comprehensive comparison among different class of PCMs.

Table 1

Comparison of thermophysical properties of different PCMs [4]

Property of Characteristics	Paraffin Wax	Non-Paraffin Organics	Hydrates Salts	Metallic
Heat of Fusion	High	High	High	Medium
Thermal Conductivity	Very Low	Low	High	Very High
Melting Temperature (°C)	-20 to +100	5 to +120	0 to +100	150 to +800
Latent Heat (kJ/kg)	200 to 280	90 to 250	60 to 300	25 to 100
Corrosiveness	Non-Corrosive	Mildly Corrosive	Corrosive	Varies
Thermal Cycling	Stable	Elevated temperature can cause decomposition	Stability/instability depends on the corresponding solid-liquid phase diagram	Stable

Paraffin, a mixture of mostly straight chain n-alkanes with general formula of $CH_3–(CH_2)_n–CH_3$ is probably the most common and widely used organic PCMs in many TES applications. Paraffin waxes which are chemically compatible with most metals owing to the characteristics of large latent heat of fusion, high storage density, minimal tendency to super-cooling, desirable thermal and chemical stability, low vapor pressure of the liquid phase, non-toxic, noncorrosive, and relatively low price [10, 13]. These clearly merit paraffin wax's utilization in TES applications for broad range of temperatures. In solar thermal systems, paraffin as a thermal energy reservoir (TER) absorbs thermal energy as heat during the day time (called charging process) when solar energy is accessible in sufficient amount and release the thermal energy over the night (called discharging process) [14]. Despite all its advantages, low thermal conductivity of paraffin wax (0.21–0.24 W/m K) can be a drawback in solar and high power applications that significantly decelerates the energy charging/discharging rates [2, 13]. Researchers tried to improve the effective thermal conductivity of paraffin and other popular PCMs using various approaches.

Dispersing high thermal conductive particles, such as carbon, metals, or graphite within PCMs was one of the approaches. Graphite usually improves thermal conductivity of paraffin in various forms such as expanded filler, or nanoparticle [15]. Earlier efforts investigated the enhancement of the heat transfer between PCM and heat transfer fluid using stationary, highly thermal conductive pieces like stainless steel and copper as well as graphite–PCM composite as an additive into PCMs [16]. The results of this research demonstrated that graphite and copper both successfully elevated the heat flux. However, stainless steel had only limited contribution. Mills et al. [17] indicated that thermal conductivity of paraffin/expanded graphite composites was enhanced by 20 to 60 times. Chen et al. [18] managed to analyze the energy storage process of a solar collector with an integrated porous structure filled with paraffin as the phase change medium. These solutions not only increase the cost of PCMs, but also solid particles loaded to enhance thermal properties reduce the amount of PCM that can be used in a fixed volume [3]. There is a recent tendency of employing various nanoparticles as thermal enhancement additives into PCMs instead of bulky metal pieces and particles. Upon the review by Khodadadi et al. [19], a wide range of nanostructure materials are utilized as thermal conductivity promoters. These include carbon-based nanostructures (nanofibers, nanoplatelets and graphene flakes), carbon nanotubes, both metallic (Ag, Al, C/Cu and Cu) and metal oxide (Al_2O_3, CuO, MgO and TiO_2) nanoparticles and silver nanowires. Authors concluded that carbon-based nanostructures exhibited far greater thermal conductivity enhancement compared to metallic/metal oxide nanoparticles. In recent decade, carbon nanotubes (CNTs) were utilized to increase effective thermal conductivities of paraffin wax and other organic PCMs [20-22]. Multi-walled carbon nanotubes (MWCNTs) showed excellent potential for heat transfer applications [22]. Wang et al. [23] added 2 wt.% of carbon nanotubes to paraffin and showed that thermal conductivity was increased by 35 and 40%

in solid and liquid states, respectively. Increment of 13% of thermal energy storage capacity of paraffin was obtained with adding 1% carbon nanotubes [3]. Reduction of melting temperature and improved thermal energy storage were reported with the loadings of MWCNT in paraffin wax [24]. Tang et al. [25] reported the enhancement of thermal storage by more than 10% for paraffin wax by loading of 1 and 5 wt.% f-MWCNT, whereas the loading of 10% of f-MWCNT decreased the thermal storage value. Some researchers reported that there is no change in thermal storage value for organic phase change materials with the presence of CNTs and xGNP (graphene nanoplatelets) [26, 27]. However, most of the studies reported a significant reduction in thermal storage for organic phase change materials with the loading of the nanoparticles [28-31].

Recently, a new family of two-dimensional materials consist of transition-metal carbides and/or carbonitrides so-called "MXene" was manufactured via selective etching out the "A" layers from $M_{n+1}AX_n$ phases (where M is an early transition metal, A is an A-group element, X is C and/or N, and n = 1, 2, or 3) and was first introduced by Naguib et al. [32] in 2011. Due to outstanding physicochemical properties such as hardness, hydrophilic nature, excellent oxidation resistance, high thermal and electrical conductivity, high thermal stability and high surface area of MXene, it has been applied in different applications [33]. MXenes have recently gained extreme attention in many exciting applications including ion batteries [24], hydrogen storage [25], water splitting [26], electronic devices [27], and supercapacitors [28]. However, MXene nanoparticle has not been explored in thermal energy storage systems and heat transfer applications yet. Specifically, there is no study on the specific heat capacity, thermal conductivity and thermal stability of PCM with MXene. The present experimental work provides a systematic approach to demonstrate the energy storage and thermal conductivity analysis of paraffin wax induced with MXene nanoparticles. This study will be useful in thermal energy storage applications. Therefore, comprehensive

investigation should be carried in this area to evaluate its full potential in thermal energy and heat transfer areas.

2. Preparation of Nanocomposite (PCM/MXene)

2.1. Materials

Organic phase change material (PLUSICE A70) with melting point of 70 °C, density of 890 kg/m^3, volumetric heat capacity of 154 MJ/m^3 and specific heat capacity of 2.2 kJ/kg K (at 25 °C) was procured from Phase Change Materials Products Ltd Company [34]. PLUSICE A70 is also known as Paraffin Wax, PW70.

2.2. Preparation of MXene (Ti_3C_2)

In the synthesis of Ti_3C_2, the following materials were used without any further purification: Ti powder (-325 mesh, 99% purity, Alfa Aesar), aluminium powder (-100+325 mesh, 99.5% purity, Alfa Aesar), titanium carbide powder (-325 mesh, 98% purity, Sigma Aldrich), sodium fluoride (99% purity, Alfa Aesar), hydrochloric acid (37.5% wt., Sigma Aldrich), and sodium hydroxide (97% purity, pellets, Sigma Aldrich). The precursor MAX phase Ti_3AlC_2 is synthesized using a molar ratio of 1:1.2:2 of (Ti:Al:TiC) elemental powders, mixed with a pestle and mortar, followed by a thermal treatment using a tube furnace under Ar atmosphere at 1,400 °C for 2 h (5 °C /min heating/cooling rate). For the etching, 4.85 g of NaF is mixed in 30 ml HCl (6 M) until dissolved. Then 3 g of Ti_3AlC_2 are slowly added to avoid overheating (it is an exothermic reaction), and the solution is left to stir at 40 °C for 48 h. After etching is complete, a dilute solution of NaOH was added slowly until the pH of the solution reached 6, and then filtered and rinsed several times with deionized water. The materials were then treated in 0.5 NaOH solution for 3 h at room temperature and filtered. The materials were then washed with deionized water, being subsequently dried at 60–70 °C overnight.

151 2.3. Preparation of PW70/MXene as a new class of nanocomposites

152 Three different concentrations of Ti_3C_2 (0.1, 0.2 and 0.3 wt.%) are loaded into the PW70. Mass
153 values of PW70 (59.940 g) and MXene flakes (0.06 g) are measured separately using microbalance
154 (Explorer series, EX224, Ohaus) with measuring uncertainty of ±0.0001. These amounts are used
155 to prepare the PW70/MXene with a 0.1 wt.% of MXene. The proposed amount of paraffin wax
156 (59.940 g) is heated in a beaker (150 ml volume) using a hot plate (RCT BASIC, IKA). The
157 temperature of hot plate is adjusted to 100 °C. PW70 is left for 15 minutes on the hot plate for
158 melting and homogenization purpose. Afterwards, 0.06 g of MXene flakes is added to the beaker
159 and stirred by a magnetic stirrer at 500 rpm. During the mixing process, the beaker is covered with
160 an aluminum foil to prevent the formation of air bubbles during magnetic stirring process. Stirring
161 process is conducted for 2 h continuously. The resultant PW70/MXene nanocomposite is poured
162 into a vial (14 ml NEST) to mold at room temperature. Same protocols are repeated to prepare
163 nanocomposites with concentrations of 0.2 and 0.3 wt.% MXene respectively by adding 0.12 and
164 0.18 g of MXene flakes as fillers to the melted organic phase change material (PW70) of 59.880 g
165 and 59.820 g, respectively.

166 **3. Characterization techniques**

167 3.1. Structural Characterization of pure MXene (Ti_3C_2)

168 3.1.1. Powder x-ray diffraction (XRD) of pure MXene (Ti_3C_2)

169 X-ray diffraction is carried out in a Smart lab diffractometer (Rigaku, Tokyo, Japan) using Cu
170 Kα radiation operating in reflection mode with Bragg-Brentano geometry to investigate the crystal
171 structure. Prior to the XRD characterization, all samples are dried in a heated oven for 18 h at
172 80 °C. The black powders are then ground and placed on a silica sample holder and pressed flat
173 with a glass slide.

174 3.1.2. Raman spectroscopy of pure MXene (Ti_3C_2)

175 Raman spectroscopy is carried out on a Horiba Lab Raman Spectrometer (Horiba, Minami-ku
176 Kyoto, Japan) with an EM-cooled Synapse camera. For taking spectra, a 100x, 0.90 NA
177 microscope objective is used. The dried powder is sandwiched between two glass microscope
178 slides which are pressed together to give flat MXene particles. One of these slides is then discarded
179 with the other slide placed flat under the diode laser (532 nm, 200 μW) for measurements.

180 3.1.3. Scanning Electron Microscopy (SEM) of pure MXene (Ti_3C_2)

181 Scanning electron microscopy is done in a JEOL JSM-7800F (JEOL, Tokyo, Japan), using an
182 accelerating voltage of 10 kV and a working distance of 10 mm, which are used to study the
183 morphology and particle size. The dried powder samples are dry cast onto a carbon tape support,
184 which is placed onto a copper stub for analysis.

185 3.2. Thermal Conductivity Measurement

186 Thermal conductivity of the pure PW70 and PW70/MXene samples are measured using a KD2
187 Pro thermal properties analyzer (Decagon, USA, version 5). This probe works with the principle
188 of a transient hot wire technique. The TR-1 sensor (100 mm length, 2.4 mm diameter) is used for
189 the thermal conductivity measurement. A programmable digital water bath (Wisd, 11Lit, WB-11)
190 with temperature accuracy of ±0.1 °C and heating power of 1 kW is used for controlling the
191 temperature within ±1 °C. Thermal conductivity of the nanocomposites (PW70/MXene) is
192 investigated at average temperature of ~25 °C. The 14 ml vial consisting of the nanocomposite
193 and sensor is placed inside a double wall beaker (1000 ml volume) covered with Styrofoam to
194 prevent the exchange of heat between sample and atmosphere. Those are wrapped using an
195 aluminum foil to prevent the formation of air bubbles during the measurements. A schematic for
196 the measurement set up for thermal conductivity is shown in Figure 2. The deviation of the

measured temperature is considered around ±0.5 °C. Each measurement is repeated three times to get the precise results. Since the temperature uniformity is highly important for the KD2 Pro, sample and sensor are allowed to achieve the temperature equilibrium for 30 minutes before any measurement is made. Reading time of the measurements is raised to 10 minutes for each measurement to ensure the accuracy of thermal conductivity results as well as reducing the error points indicated by decagon instrument.

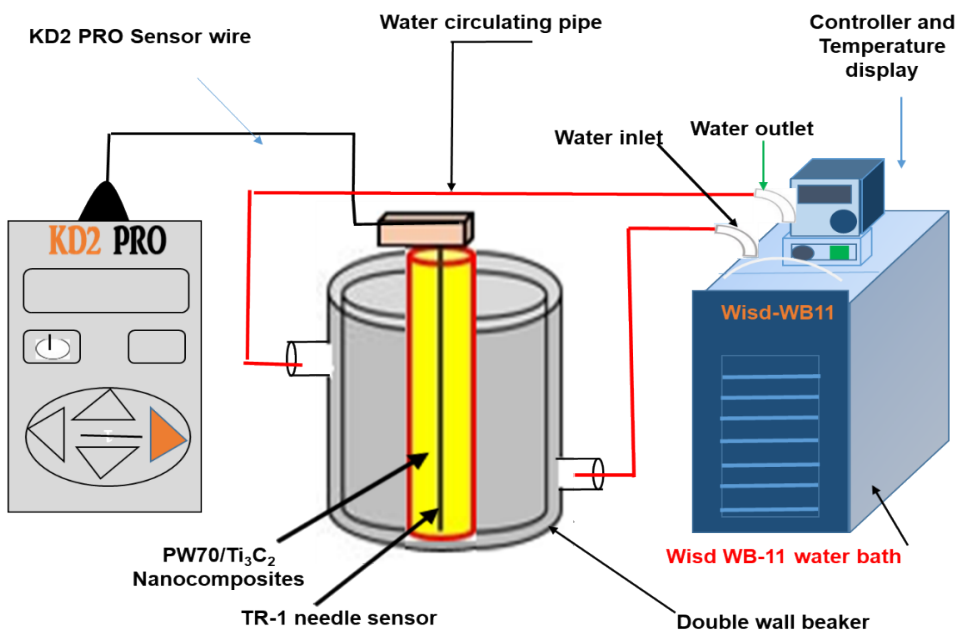

Figure 2. Thermal conductivity measurement set up for nanocomposites

3.3. Specific heat capacity (c_p) measurement

In this study, the specific heat capacity (c_p) measurements of PW70/MXene nanocomposite samples are performed using a differential scanning calorimetry (DSC). DSC-1000/C (Linseis, Germany) is a high resolution (0.03μW) instrument and the measurements are conducted using an aluminum crucible of 40 μl. The temperature range for measurements is between 25-250 °C with the heating rate of 10 °C/min. The nanocomposite samples are tightly sealed in a regular aluminum crucible with the capacity of 40 μl under a nitrogen atmosphere with a flow rate of 20 ml/min. The

212 temperature repeatability and calorimetric precision are ±0.1°C and ±1%, respectively.
213 Temperature and enthalpy calibrations for this DSC are carried out employing four standard
214 reference samples (Indium, Tin, Lead and Zinc) provided by the supplier. The experimentally
215 achieved data for specific heat capacity value of the pure paraffin wax is found in good agreement
216 with c_p value provided by the supplier. One uniform protocol for c_p measurements of the
217 PW70/MXene nanocomposites are adjusted in order to ensure the accuracy of results. All DSC
218 measurements are performed using the heating rate of 10 °C/min under nitrogen atmosphere.

219 3.4. Thermal stability test

220 Thermogravimetric analysis (TGA) of the PW70/MXene nanocomposites are conducted using
221 Perkin Elmer TGA 4000. A 180 µl alumina crucible (withstanding temperature ~1750 °C) under
222 an ultra-high pure nitrogen gas flow of 19.8 ml/min with the gas pressure of 2.6 bar is selected to
223 examine the samples. The utilized heating rate is 10 °C/min for raising the temperature from 30 to
224 800 °C. About 15 mg of PW70/MXene nanocomposite sample is used for the decomposition
225 temperature measurement. The obtained data is analysed using Pyris Software.

226 3.5. Fourier transform infrared spectrum (FT-IR)

227 The Fourier Transform Infrared spectrum (FTIR) of the PW70/MXene nanocomposites is
228 determined using a Perkin Elmer Spectrum Two-UATR. Spectra is detected using the integrated
229 detector of MIR TGS (15000 - 370 cm^{-1}). Scanning speed is 0.2 cm/s within the optimum scan
230 range of 500 - 4000 cm^{-1}.

231 3.6. Ultraviolet-visible (UV-Vis) spectroscopy

232 Optical absorbance measurements are performed using Ultraviolet-visible (UV-Vis). Spectra is
233 acquired using Perkin Elmer Lambda 750. Data is collected at room temperature within the

wavelength from 800 to 200 nm. The adjusted scan speed is 266.75 nm/min with the 860 nm monochromator.

3.7. HRTEM and elemental analysis of MXene nanoparticles

Morphology of the MXene flakes is investigated using HRTEM (JEOL JEM-ARM 200F) imaging at an accelerating voltage of 200 kV. About 1 mg of MXene flake is added into ~ 4 ml of ethanol in a vial. The mixture is remained on the hot plate at 60 °C and stirred using a magnetic stirrer for half an hour. About 4 µl of diluted sample is taken by micropipette and dripped onto the carbon-coated cupper grid. Energy dispersive X-ray spectroscopy (EDX, OXFORD INSTRUMENT) is used to confirm the elemental map imaging and observation of spatial distribution of all the elements. The spot analysis is carried out to detect the quantitative distribution of elements in different portions of MXene.

4. Results and Discussion

4.1. Structural characterization of pure MXene (Ti_3C_2)

To confirm the structure of the as-synthesized MXene, XRD, Raman spectroscopy and SEM studies are carried out and results are presented in Figure 3. The XRD data shows a sharp diffraction peak at 7.1˚ 2θ, corresponding to the (002) diffraction plane (Figure 3b). This gives an interlayer spacing of 14.5 Å, consistent with previous reports of HCl-fluoride salt etched Ti_3C_2 [35]. Other (00l) diffraction peaks such as (004) and (008) are also present, confirming the successful synthesis of MXene (Ti_3C_2). Raman spectroscopy also confirms the formation of Ti_3C_2 with the Raman Spectra matching previous reports [36, 37]. The peaks at 207 cm^{-1} and 270 cm^{-1} correspond to E_g vibrations resulting from the presence of Ti-O and Ti-OH surface groups, respectively. The broad peaks which center around 390 cm^{-1} and 580 cm^{-1} are known to result from vibrations relating to the presence of Ti-O, Ti-OH and Ti-F groups, all of which are common

surface terminations for MXene (Ti_3C_2) [36, 37]. SEM characterization reveals that the as-synthesized MXene flakes are multilayered, with particle sizes ranging from 1-10 µm. The layered nature of the MXene is also noticed, and matches previous reports [35].

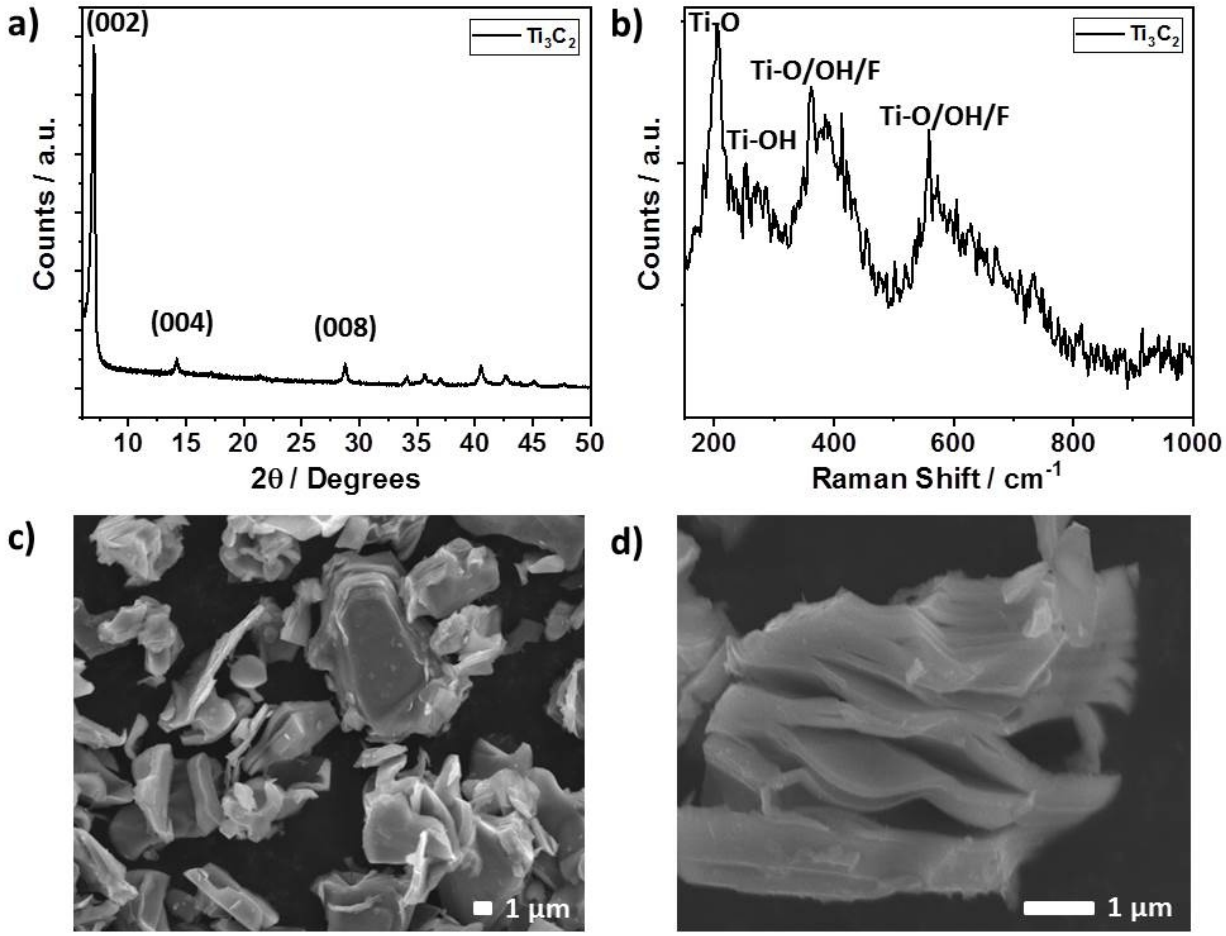

Figure 3. Structural characterization of the as-synthesized MXene (Ti_3C_2). a) XRD diffractogram b) Raman spectrum c-d) SEM micrographs at different magnifications.

4.2. Morphological characterization of MXene (Ti_3C_2)

An overview of emerging layered structure of MXene (Ti_3C_2) can be seen in Figure 4 where a high-resolution TEM (HRTEM) image of few layered Ti_3C_2 flake is shown covering in a whole carbon TEM grid. A low magnification image in Figure 4(a) depicting the electron-transparent

thin morphology and a few layer structures. Moreover, the thin MXene nanosheet is presented to be flexible and foldable which is similar to those of graphene and two-dimensional MXenes [32, 38]. Its Fast Fourier Transform (FFT) (Figure 4.b) reveals a hexagonal-based crystal with chain-like features of the MXene nanosheets [38]. The delaminated layers are found to be transparent to the electron beam in TEM. Selected area electron diffraction (SAED) of delaminated MXene (in Figure 4.c) image clearly shows that the atomic arrangement in the basal planes is identical to that in the parent MAX phase [39]. These results provide further convincing evidence for the three-dimensional to two-dimensional conversion of the material. Furthermore, it is clear from TEM observation that there is no evidence for carbide amorphization. Ti_3C_2 sheets are found to be more stable than graphene sheets under a 200 kV electron beam in the TEM [39, 40]. EDX results of the same MXene flake confirm the presence of Ti, C with minor amounts of F, and O from the MXene surface and very small amount of Al. Analysis of the intensity profile along the right dashed line (Figure 4.d) gives the Ti-C bond length of ~ 2.11 Å close to the expected value of 2.089 Å [41].

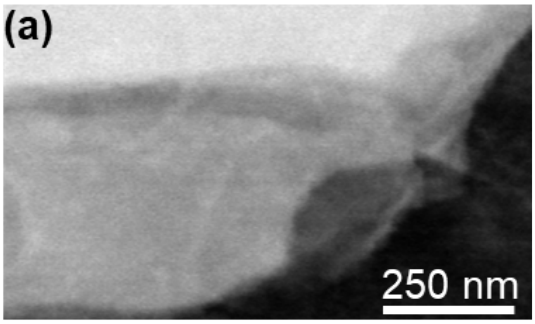

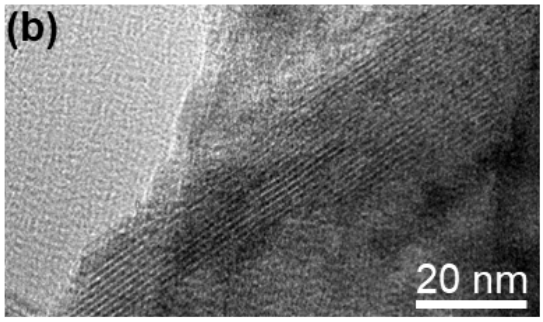

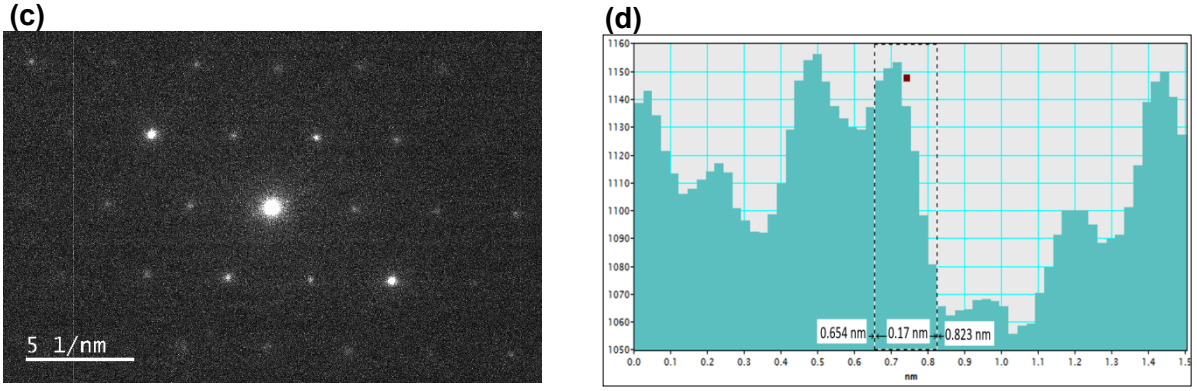

Figure 4. Top view of typical bright-field HRTEM images of the of a MXene (Ti_3C_2) flake. (a) low-magnification image of few layered MXene flake, (b) higher magnification HRTEM image of edge-on MXene (Ti_3C_2), (c) corresponding to the selected area electron diffraction pattern, (d) intensity analysis along the white dashed line shows Ti-C bond length of 2.11 Å.

4.3. Chemical structure characterization (FTIR) results

The chemical structures of the pure organic paraffin wax and the synthesized PW70/MXene nanocomposites are investigated using FTIR spectroscopy analysis. The achieved FTIR spectrum is presented in Figure 5. The FTIR spectrum for PW70/MXene nanocomposites and pure PW70 is shown separately. Inset of the Figure 5 presents the FTIR spectrum of pure MXene used in this work showing the peaks for Ti-O at ~530 cm^{-1} and prominent peak for O-H group at ~3250 cm^{-1} from the intercalated water in the MXene. On the other hand, shifts in the characteristic peaks of PCM/MXene nanocomposites revealed the presence of C-O-C, O-H, C=C, C-O and C-H groups in the samples. The peak at 2924 - 2960 cm^{-1} corresponds to the skeletal vibrations from C-O, C-H and O-H groups in the MXene structure. The presence of oxygen functionalities in the samples is detected in peaks at 1380 cm^{-1} due to O-H stretching vibrations. There is no O-H band detection in the wavenumber of 3400 cm^{-1} [42, 43]. Besides, it's observed peaks for C-C-C and C=C at ~721 and ~1466 cm^{-1} respectively, is allocated due to the stretching deformation vibration of intercalated

water in the MXene sample [44]. Clearly, it is seen that the wavenumbers (cm^{-1}) of characteristic peaks of all the composite samples with varying MXene loading mass fraction is similar. It reveals that due to the increase of MXene in this low amount (wt.%) in the PCM, negligible chemical changes occurred in the PCM. A few extra peaks have been observed at ~721 and ~1466 cm-1 in the characteristic FTIR spectrum of the pure PW70 beyond the effect of MXene addition indicating the purity of the PCM (PW70).

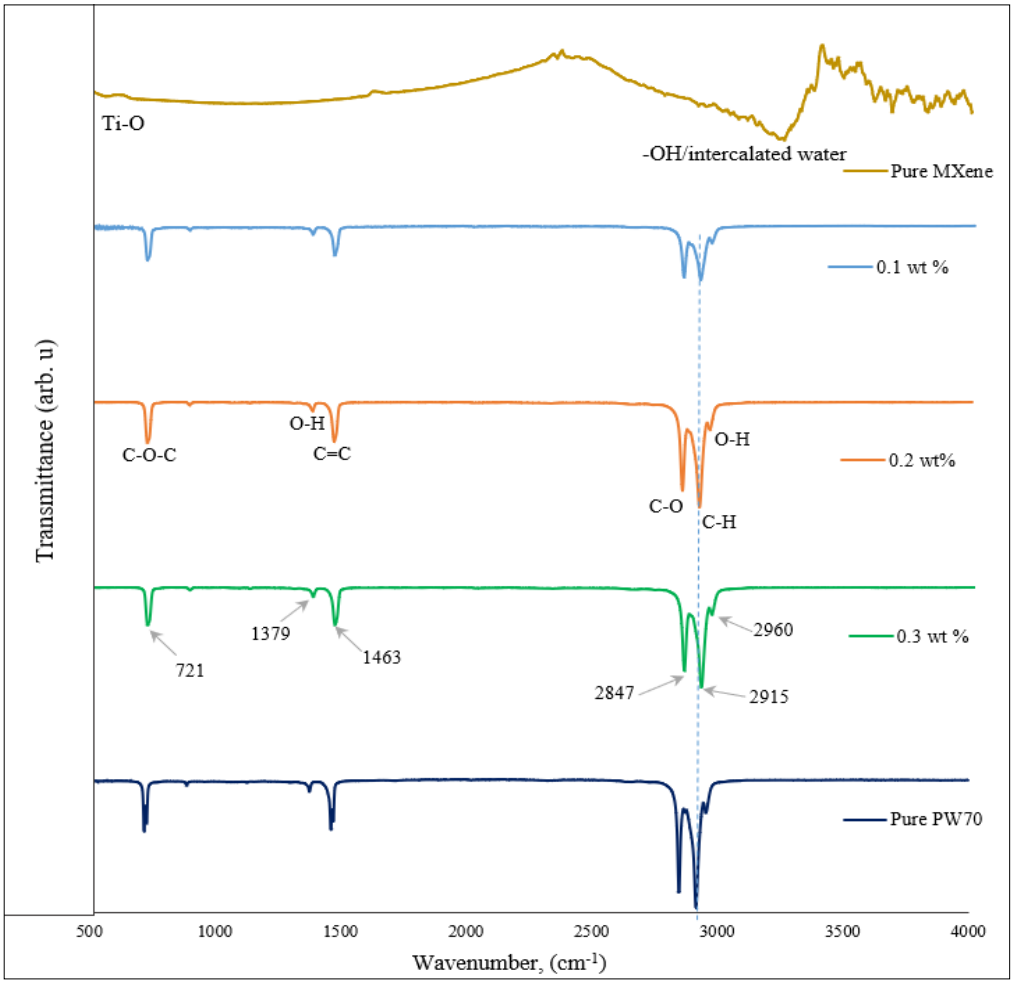

Figure 5. Full range (500 - 4000 cm^{-1}) FTIR spectra of pure MXene and PW70/Ti_3C_2 nanocomposites with varying MXene loading mass fraction and base material of pure PW70 PCM.

4.4. UV-Vis absorption spectrum characterization

The conversion of abundant solar energy into usable energy is an important point regarding phase change materials which makes the possibility of storing energy during exposure to sunlight and utilize at night. This kind of energy storing is called adsorptive energy storage that can be measured through Ultraviolet-visible spectrometry (UV-Vis) in different wavelengths. UV-Vis spectrometry of the PW70/MXene as a new class of nanocomposites is carried out by using Lambda 750 Perkin Elmer. Absorbance measurements are achieved through optical resolution of 0.4 nm and over wavelength of 200-800 nm. The typical optical absorption spectra of pure organic paraffin wax and PW70/MXene nanocomposite samples with different mass fractions of 0.1, 0.2 and 0.3 wt.% are measured and presented in Figure 6. Standard deviation of absorbance's of the three repeated measurements of the pure PW70 and PW70/MXene nanocomposite samples with varying wt.% of MXene are presented at the inset of the Figure 6. Pure PW70 spectrum has the characteristic maximum at 200-300 nm region which is consistent with the literature data [45]. The peak that appears at 230 nm in the UV–Vis spectrum of PW70 contributed to the degree of the remaining conjugation (π- π^* transition), and the shoulder around 300 nm should be ascribed to the n-π^* transition of carbonyl groups. The absorbance in the 270-350 nm regions is thought to be caused by the conjugated aromatic domains [46]. Pure organic paraffin wax shows two absorption peaks in the UV light range. However, almost no absorption peak is seen in the visible light range (350-800 nm). The high background adsorption in the visible light range is induced by the scattering of crystalline paraffin [46]. The UV-Vis spectra of PW70/MXene nanocomposites exhibit typical absorption peaks at 220 and 290 nm which is consistent with the literature data [47]. It is seen that pure PW70 and PW70/MXene nanocomposite sample with 0.1 wt.% show similar patterns with slight shifting of wavelength. The absorbance of the prominent peaks is found to be

increased about ~14% over pure PW70. On the other hand, PW70/MXene nanocomposite samples with 0.2 and 0.3 wt.% show the prominent peaks more consistent with MXene [46]. However, absorbance for these compositions are increased about ~38 and ~39% over pure organic paraffin wax. Thus, through the experimentally achieved data, it is evident that using MXene nanoparticles as additives to conventional PCMs can affect the intermolecular dynamics. The intermolecular interactions between atoms in surface area of MXene nanoparticles and C-H bonds of the organic phase change materials may cause to enhance the light-to-heat energy conversion [48]. The achieved enhancements in the absorbance of the prepared novel PW70/Ti_3C_2 nanocomposites might attribute to improve the efficiency of the solar systems by incorporating nanocomposites integrated with optical layers during direct exposure to sunlight

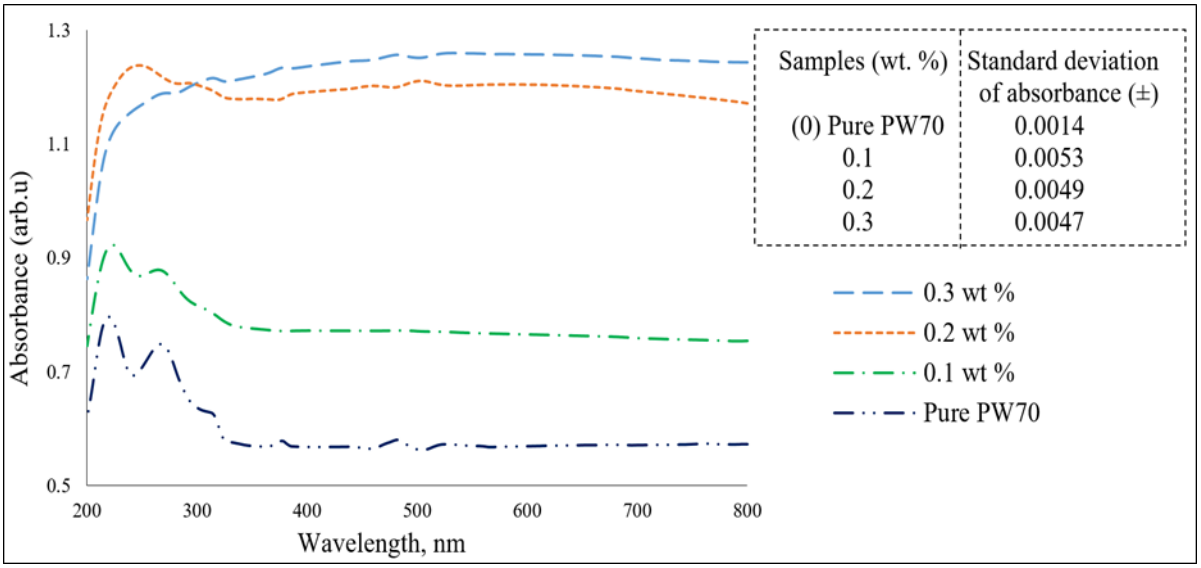

Figure 6. UV-Vis spectra of pure PW70 and PW70/MXene nanocomposite samples. Inset: standard deviation of absorbance

4.5. Thermal conductivity of organic PCM dotted with MXene (Ti_3C_2)

Thermal conductivity is an important determinant for PCMs, influencing the rate of thermal energy charging/discharging throughout the day/night. Table 3 illustrates experimentally achieved data of thermal conductivity for nanocomposites with different loadings of MXene (Ti_3C_2) flakes including the average value of thermal conductivity for three data points. The experimentally obtained data reveals that the thermal conductivity of pure paraffin wax is found to be ~0.2 W/mK which is in good agreement with literature value of 0.21 W/mK [49]. The thermal conductivity of PCM/MXene nanocomposites increases by approximately 6.1, 12.4 and 16% for a loading concentration of 0.1, 0.2 and 0.3 wt.%, respectively. The achieved average error point for three different readings of pure PW70 is ± 0.007. Low error points proved the accuracy of the thermal conductivity measurements. It is observed that the addition of MXene into PW70 remarkably improved the nanocomposite's thermal conductivity. The enhancement can be attributed to the greater thermal conductivity of MXene at higher mass fractions in addition to the high surface area-to-volume ratio of MXene compared to that of paraffin wax. Nevertheless, the thermal resistance at the interface between MXene and PW70 could not be neglected. The previous studies have proved that the thermal boundary resistance rises up remarkably as the nanoparticle dimensionality escalates based on the results for two-dimensional materials included graphene nano platelets [50]. Enhancement in thermal conductivity in the PW70/MXene nanocomposites is more likely due to the high surface area and negligible thickness of MXene flakes. This reason might contribute to create a percolation conducting network in the PCM matrix.

Table 3
Experimentally achieved data for thermal conductivity measurement using KD2 Pro Decagon

Nanocomposite (PW70/MXene)	Thermal Conductivity (W/mK)		Temperature (°C)	
	Average value	Standard deviation	Average value	Standard deviation
Pure PW70	0.197	0.004	25.42	0.42
PW70/MXene (0.1 wt.%)	0.209	0.007	25.19	0.19
PW70/MXene (0.2 wt.%)	0.221	0.010	25.27	0.27
PW70/MXene (0.3 wt.%)	0.228	0.013	25.26	0.26

According to Yang et al. [50], 1 wt.% Nano-Si_3N_4 additives escalated the effective thermal conductivity of paraffin wax by ~10% at room temperature. Li et al. [51] utilized MWCNTs in synthesizing phase change microcapsules (MicroPCMs) compromised paraffin wax in order to enhance the thermal conductivities of the microcapsules. The results indicated that thermal conductivity of MicroPCMs/CNTs-SA with 1% of CNTs increased by ~19% compared with that of MicroPCMs. In another study, Wang et al. [24] investigated the influence of adding MWCNTs to the thermal properties of paraffin wax (PW). The PW/MWCNT composites showed no lamination after settled for 96 h at liquid state. It was observed that for the PW/MWCNTs binary nanocomposites with a weight fraction of 0.2, 0.5 and 2%, the thermal conductivity enhancement reached ~11, 16 and 35% in solid state at 30 °C, respectively. The superior performance of our synthesized MXene in raising the thermal conductivity of PCMs compared to above-mentioned past results may be attributed to their particular planar structure and two-dimensional geometry. As proposed by the molecular dynamics simulation data of Tang et al. [25], the improvement in

effective thermal conductivity is not only owing to the presence of the highly-conductive nanofillers, but is also owing to the filler-induced alignment of the paraffin molecules that inherently raises the thermal conductivity of the matrix.

4.6. Thermal energy storage characteristics of the pure paraffin and PW70/MXene (Ti_3C_2)

For the purpose of assessment, calculation and design of thermal systems, specific heat capacity is considered as one of the major parameters [52]. Thermal energy performance of the pure organic paraffin wax and PW70/MXene nanocomposites are examined using DSC. Distinct solid to liquid phase change peeks can be observed in Figure 7. Table 4 presents the all achieved data for c_p measurements of pure organic PCM and PW70/MXene nanocomposites.

Table 4

Experimentally acquired data for c_p measurements of pure paraffin wax and PW70/MXene nanocomposites

Samples	Specific heat capacity (J/g K))	
	Temperature (°C)	
	Low temperature (~25 °C)	High temperature (~250 °C)
Pure paraffin wax	2.1	3.11
PW70/MXene (0.1wt.%)	2.2	3.31
PW70/MXene (0.2wt.%)	2.2	4.03
PW70/MXene (0.3wt.%)	2.8	4.43

The experimentally achieved DSC results of pure paraffin wax and PW70/MXene nanocomposites for specific heat capacity measurements are presented in Figure 7.

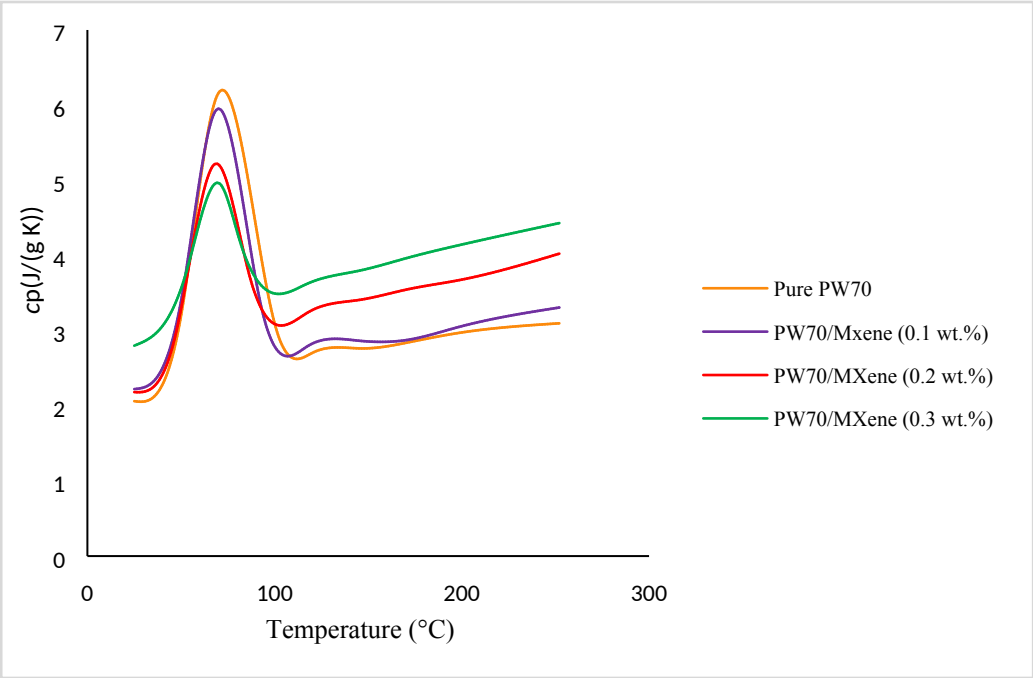

Figure 7. DSC diagrams of pure PCM and PW70/MXene nanocomposites: c_p measurement of pure paraffin wax and PW70/MXene nanocomposites.

Figure 7 demonstrates the phase transformations for pure organic PCM and PW70/MXene nanocomposites. DSC diagrams indicate that c_p values for pure organic paraffin wax in the temperatures of ~25 and ~250 °C are 2.1 and 3.10 (J/g K), respectively (Table 4). Acquired experimentally data for c_p value (2.1 J/g K) of the pure paraffin wax at 25 °C is in good agreement with the provided data by supplier (2.2 J/g K) [34]. In a research work conducted by Christoph Hilgert et al. [53] under a comprehensive project (SFERA II project), the authors investigated the uncertainty of c_p measurements. They reported uncertainty of the c_p measurement in the value of 1.3 % at mean operation temperatures between 25 and 60 °C. The uncertainty measurement in the present work is in the range of ~3 % which is based on the higher operating temperature (up to ~250 °C). In another research work, Bingham [54] reported uncertainty measurement of c_p value in the range of 4.5-6 %. As it is clear from the achieved data that the c_p value increases for pure PCM at elevated temperatures. The mechanism for increasing specific heat capacity at elevated

412 temperatures can be described due to vibrational, rotational and translation of molecules at higher
413 temperatures. Heating up a substance will cause to increase the average energy of molecules which
414 will lead to store more amount of energy [48]. Acquired data from Figure 7. illustrates that the
415 changes of c_p value for PW70/MXene (0.1 wt.%) in low temperature (~25 °C) is negligible (c_p=2.2
416 J/g K)). The increment of c_p value at high temperature (~250 °C) is ~7%. The DSC results for
417 PW70/MXene (0.2 wt.%) indicate small changes of c_p value (c_p= 2.2 J/g K)) in low temperature
418 (25 °C). However, enhancement of ~29.5% was achieved in high temperature (~250 °C) for the
419 nanocomposite with 0.2 wt.% loading of MXene flakes. The achieved data for c_p values of
420 PW70/MXene (0.3 wt.%) reveals ~34% enhancement of c_p value at low temperature (25 °C) and
421 ~43% increment of c_p value at high temperature (~250 °C).
422 Literature reports express that specific heat capacity of nanocomposites can be increased up to
423 25% compared with the base substance due to the presence of nanoparticles [55]. Wang et al. [24]
424 applied a theoretical model to report that the c_p value of nanoparticles can be enhanced when the
425 size of nanoparticles is decreased. Less number of bonds in the surface area of the lattice of the
426 nanoparticles causes the atoms to be less constrained. Lower natural frequency and higher
427 amplitude of the vibrations of the atoms in the surface area can allow the bonds to act like spring.
428 This phenomenon can be the cause of creation of interface interaction of atoms in surface area of
429 two-dimensional materials (because of high surface area) with high surface energy atoms of the
430 organic pure paraffin (C-H bonds). The created interactions between atoms can be the reason of
431 the enhanced specific heat capacity of PW70/MXene nanocomposites. This mechanism is
432 applicable in high temperatures as the temperature elevates the vibration of atoms. Enhancement
433 of vibration will increase specific heat capacity, which is found experimentally in this study for
434 new class of nanocomposites (PW70/MXene) with different mass fraction loadings of MXene

flakes. Due to the C-H bond in the structure of organic phase change materials and high surface area of two-dimensional inorganic compound (MXene) it can be proposed that there is an electrostatic interaction between the induced MXene in PW70. The aforementioned interface interaction will cause to crystallize the particles of paraffin wax on the specific surface area of MXene. Large specific surface area and specific surface energy will contribute to the enhancement of the specific heat capacity. The acquired promising thermodynamic efficiencies at higher operating temperatures may reduce the final cost of the thermal systems which are working in the basis of thermal storage and thermal conductivity. An inexpensive method to reduce the cost of a system is to enhance the thermophysical properties of organic/inorganic phase change materials by doping them with minute concentration of nanoparticles. In a comprehensive research study performed by Malik [56], the preliminary cost models for inorganic phase change materials (alkali-salt eutectics) were investigated. In the above-mentioned study, the developed model for inorganic phase change material induced with alumina nanoparticles revealed cost-effectiveness by enhancement in the specific heat capacity value. The author demonstrated that a 30% enhancement in specific heat capacity would offer a 15% saving in solar thermal power systems. The above-mentioned model can be extended for organic phase change materials as well. Thus, based on the developed model by Malik [56], the cost-effectiveness of the PW70/MXene nanocomposites for solar thermal power systems might be expected according to the experimentally achieved improvement specific heat capacity value. The required amount of thermal energy storage media in concentrated solar power plants can be reduced significantly decrease with enhancement of the specific heat capacity value, followed by a consequent reduction in the cost of electricity.

4.7. Thermal stability of pure PW70 and PW70/MXene nanocomposites

Thermal durability of the pure organic phase change material and PW70/MXene nanocomposites has been evaluated by thermogravimetric analysis (TGA). Acquired TGA curves are presented in Figure 8. TGA analysis for all samples is followed with a unique protocol and same condition (mass value of ~14.5 mg and heating rate of 10 °C/min) to ensure the accuracy of achieved results. It was observed that there is a slight shift in initial and final degradation temperatures of the pure paraffin wax and PW70/MXene nanocomposites. The achieved data reveals that the focal degradation temperature for pure organic phase change material is found to be 362.5 °C. The presented data show that there is a slight increment in final degradation temperature of nanocomposite induced with MXene flakes. The focal degradation temperature for the nanocomposites of PW70/MXene with different loadings (0.1, 0.2 and 0.3 wt.%) is achieved 363.9, 380.9 and 384.0 °C. From figure 8. (b), it is clear that with the increased concentration of Ti_3C_2, the thermal stability of the nanocomposites is increased. The acquired data confirms that with extending the loading amount of MXene nanoparticles, the thermal durability of the PW70/MXene nanocomposites can be increased consequently.

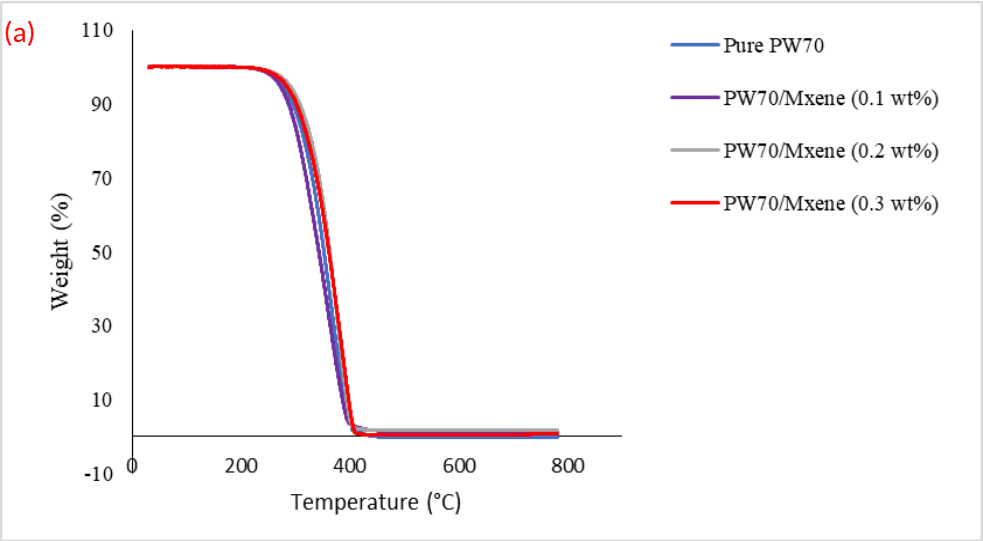

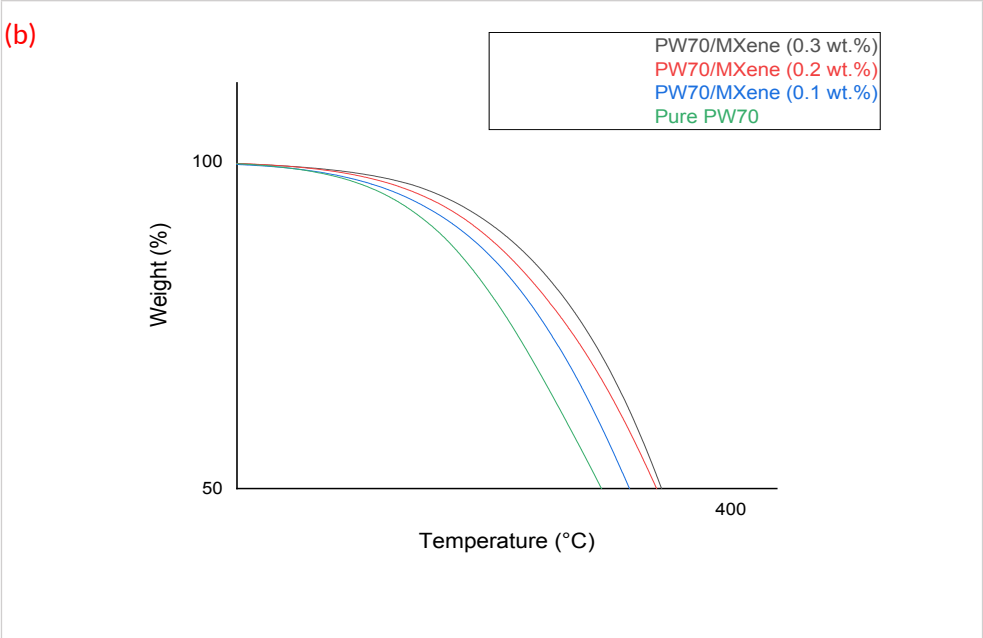

Figure 8. Thermogravimetric analysis of (a) pure organic PCM and PW70/Ti_3C_2 nanocomposites (b) enlarged area of the decomposition temperature region

4.8. Characterization of enthalpy and melting point of the PW70/Ti_3C_2

Enthalpy and melting point characterization of the synthesized PW70/MXene nanocomposites and pure PCM are performed using the DSC. Figure 9. presents the enthalpy results for pure paraffin wax and nanocomposites with different mass fractions of MXene flakes. The experimentally achieved data for melting point of pure PW70 is reported to be 69.8 °C which is in good agreement with the provided data by supplier of the pure PCM [34]. The uncertainty measurement in the value of the melting temperature is ~ 0.3%. It is observed that with adding MXene (Ti_3C_2) nanoparticles to pure paraffin wax, the melting point is increased slightly from 69.8 to 71.7 °C for the highest concentration of MXene flakes (0.3 wt.%). The slight increment can be observed because of the interface interaction between high surface energy atoms of pure paraffin wax and high surface area of MXene nanoparticles. The increment of melting point confirms the explained mechanism of enhancement in the specific heat capacity. The achieved

488 data for melting point of PW70/MXene with loading of 0.1 and 0.2 wt.% are 70.7 and 71.4 °C. It
489 is observed from the DSC curves that the endothermic enthalpy value decreases with MXene flakes
490 as additive. This shows that the releasing energy in melting point occurs and heat transfer enhances
491 in this crucial point. The experimentally acquired data for enthalpy of pure PCM is found to be
492 110.68 J/g (endothermic) which is in agreement with the provided data by the supplier (107 kJ/kg)
493 [34]. The standard deviation for the enthalpy measurement is estimated to be ~ 3%. However, the
494 achieved data for enthalpy of PW70/MXene for the concentrations of 0.1, 0.2 and 0.3 wt.% are
495 93.86, 95.15 and 99.53 J/g, respectively. The results show that lower concentration of MXene
496 flakes (0.1 wt.%) has caused to less endothermic enthalpy. This performance shows that higher
497 concentration of MXene flakes causes to create stronger crystallinity which will lead to have more
498 thermal storage at this crucial point.

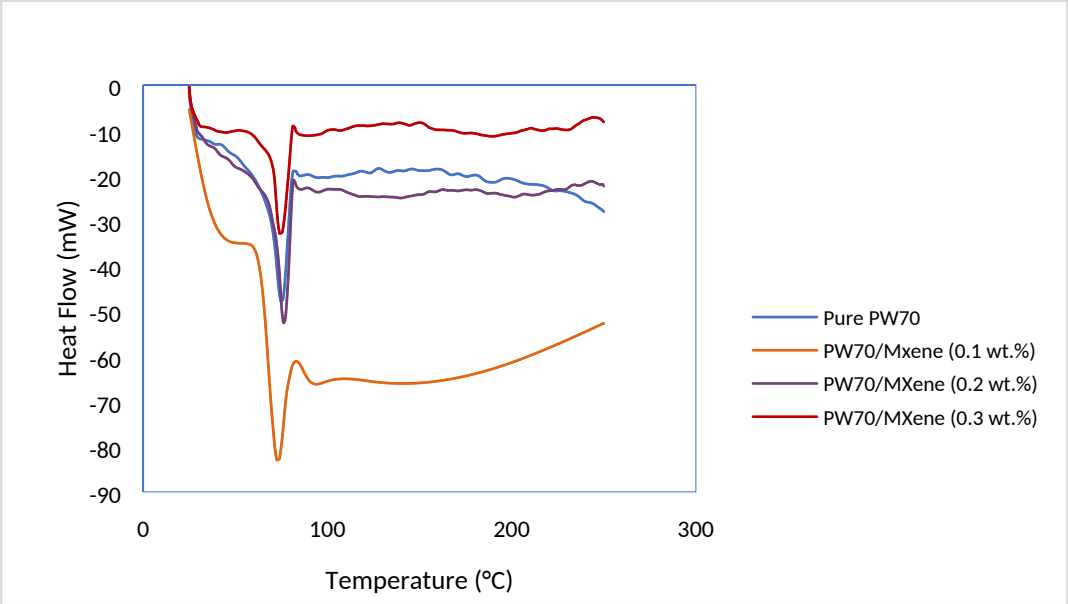

499

500 **Figure 9.** Enthalpy and melting point characterization of PW70/MXene nanocomposites and pure PCM.
501 (DSC curves)

502

5. Conclusion

In this paper, a new class of nanocomposite using MXene (Ti_3C_2) nanoparticles as additive to a pure organic phase change material has been successfully synthesized. Structural analysis of the synthesized MXene flakes has been investigated by using x-ray diffraction, Raman spectroscopy and SEM characterizations. XRD and Raman spectroscopy analysis confirm the purity of the synthesized MXene flakes. SEM characterization reveals that the synthesized MXene flakes are multilayered, with particle sizes ranging from 1-10 μm. FITR results show good formation of the synthesized nanocomposites. Thermal energy storage capability of the PW70/MXene and pure paraffin wax has been measured at elevated temperatures considering decomposition temperature as maximum operating temperature. It is revealed that the specific heat capacity of the PW70/MXene nanocomposite with mass fraction of 0.3 wt.% enhanced by ~ 43% compared to the pure PW70. Thermal conductivity of the PW70/MXene nanocomposite is found to have enhancement of 16 % with mass fraction of 0.3 wt.%. The unique two-dimensional and well-formed layers of planar structure of MXene nanomaterials leads to obtain high promising thermophysical properties. The melting point of the synthesized nanocomposite is shown to be slightly increased at elevated loadings of MXene nanomaterials. The melting point for pure paraffin is found to be 69.8 °C. Melting point of PW70/MXene with loading of 0.3 wt.% is measured to be 71.7 °C. The final degradation temperature of PW70/MXene nanocomposite in volume fraction of 0.3 wt.% is found to be 384 °C. Upon realizing the superior performance of the new emerging nanomaterials (MXene) in serving as nanofillers for preparation of PCM nanocomposites with enhanced thermal storage and thermal conductivity, the effects of the number of layers, thickness and the size are of great interest for future studies. Thermal conductivity at elevated temperature also need to be carried to investigate its variation with temperature.

Acknowledgement

"R. Saidur would like to acknowledge the financial support provided by the Sunway University through the project no# STR-RCTR-RCNMET-001-2019". The authors would like to thank Dr. Michael Naguib for useful discussion and comments.

References

1. Lewis, N.S., *Toward cost-effective solar energy use*. science, 2007. **315**(5813): p. 798-801.
2. Şahan, N., M. Fois, and H. Paksoy, *The effects of various carbon derivative additives on the thermal properties of paraffin as a phase change material*. International Journal of Energy Research, 2016. **40**(2): p. 198-206.
3. Sahan, N. and H.O. Paksoy, *Thermal enhancement of paraffin as a phase change material with nanomagnetite*. Solar Energy Materials and Solar Cells, 2014. **126**: p. 56-61.
4. Sharma, A., et al., *Review on thermal energy storage with phase change materials and applications*. Renewable and Sustainable energy reviews, 2009. **13**(2): p. 318-345.
5. Lorsch, H.G., K.W. Kauffman, and J.C. Denton, *Thermal energy storage for solar heating and off-peak air conditioning*. Energy conversion, 1975. **15**(1-2): p. 1-8.
6. Nithyanandam, K. and R. Pitchumani, *Optimization of an encapsulated phase change material thermal energy storage system*. Solar Energy, 2014. **107**: p. 770-788.
7. Wu, S. and G. Fang, *Dynamic performances of solar heat storage system with packed bed using myristic acid as phase change material*. Energy and Buildings, 2011. **43**(5): p. 1091-1096.
8. Mukhtar, A., et al., *Performance Assessment of Passive Heating and Cooling Techniques for Underground Shelter in Equatorial Climate*.
9. Miao, W., et al., *Development of spherical α-Al2O3-based composite phase change materials (PCMs) and its utilization in thermal storage building materials*. Thermochimica Acta, 2019. **676**: p. 177-185.
10. Li, M., Q. Guo, and S. Nutt, *Carbon nanotube/paraffin/montmorillonite composite phase change material for thermal energy storage*. Solar energy, 2017. **146**: p. 1-7.
11. Soda, M. and A. Beyene, *Multiphase ultra-low grade thermal energy storage for organic Rankine cycle*. International Journal of Energy Research, 2016. **40**(1): p. 51-60.
12. Benslimane, F., F. Bounaama, and B. Draoui, *Bond Graph Modeling and Control of A Single-Zone Building in a Semi-Arid Region for Thermal Comfort*. 2019.
13. Fan, L.-W., et al., *Effects of various carbon nanofillers on the thermal conductivity and energy storage properties of paraffin-based nanocomposite phase change materials*. Applied Energy, 2013. **110**: p. 163-172.
14. Senthil, R. and M. Cheralathan, *Enhancement of the thermal energy storage capacity of a parabolic dish concentrated solar receiver using phase change materials*. Journal of Energy Storage, 2019. **25**: p. 100841.
15. Yu, Z.-T., et al., *Increased thermal conductivity of liquid paraffin-based suspensions in the presence of carbon nano-additives of various sizes and shapes*. Carbon, 2013. **53**: p. 277-285.
16. Mazman, M., et al., *Heat transfer enhancement of fatty acids when used as PCMs in thermal energy storage*. International Journal of Energy Research, 2008. **32**(2): p. 135-143.
17. Mills, A., et al., *Thermal conductivity enhancement of phase change materials using a graphite matrix*. Applied Thermal Engineering, 2006. **26**(14-15): p. 1652-1661.

18. Chen, Z., M. Gu, and D. Peng, *Heat transfer performance analysis of a solar flat-plate collector with an integrated metal foam porous structure filled with paraffin*. Applied Thermal Engineering, 2010. **30**(14-15): p. 1967-1973.
19. Khodadadi, J., L. Fan, and H. Babaei, *Thermal conductivity enhancement of nanostructure-based colloidal suspensions utilized as phase change materials for thermal energy storage: a review*. Renewable and Sustainable Energy Reviews, 2013. **24**: p. 418-444.
20. Elsayed, A.O., *Numerical study on performance enhancement of solid–solid phase change materials by using multi-nanoparticles mixtures*. Journal of Energy Storage, 2015. **4**: p. 106-112.
21. Kumaresan, V., R. Velraj, and S.K. Das, *The effect of carbon nanotubes in enhancing the thermal transport properties of PCM during solidification*. Heat and Mass Transfer, 2012. **48**(8): p. 1345-1355.
22. Bashar, M. and K. Siddiqui, *Experimental investigation of transient melting and heat transfer behavior of nanoparticle-enriched PCM in a rectangular enclosure*. Journal of Energy Storage, 2018. **18**: p. 485-497.
23. Wang, J., et al., *Increasing the thermal conductivity of palmitic acid by the addition of carbon nanotubes*. Carbon, 2010. **48**(14): p. 3979-3986.
24. Wang, J., H. Xie, and Z. Xin, *Thermal properties of paraffin based composites containing multi-walled carbon nanotubes*. Thermochimica Acta, 2009. **488**(1-2): p. 39-42.
25. Tang, Q., et al., *Improving thermal conductivity and decreasing supercooling of paraffin phase change materials by n-octadecylamine-functionalized multi-walled carbon nanotubes*. RSC Advances, 2014. **4**(69): p. 36584-36590.
26. Cui, Y., et al., *The experimental exploration of carbon nanofiber and carbon nanotube additives on thermal behavior of phase change materials*. Solar Energy Materials and Solar Cells, 2011. **95**(4): p. 1208-1212.
27. Kim, S. and L.T. Drzal, *High latent heat storage and high thermal conductive phase change materials using exfoliated graphite nanoplatelets*. Solar Energy Materials and Solar Cells, 2009. **93**(1): p. 136-142.
28. Ho, C.J. and J. Gao, *Preparation and thermophysical properties of nanoparticle-in-paraffin emulsion as phase change material*. International Communications in Heat and Mass Transfer, 2009. **36**(5): p. 467-470.
29. Halassa, D., et al., *Effect of Solar Air Flat Plate Collector Geometric Parameters on The Thermal Behavior Inside an Indirect Solar Drier*.
30. Teng, T.-P. and C.-C. Yu, *Characteristics of phase-change materials containing oxide nano-additives for thermal storage*. Nanoscale research letters, 2012. **7**(1): p. 611.
31. Dardir, M., et al., *Opportunities and challenges of PCM-to-air heat exchangers (PAHXs) for building free cooling applications—A comprehensive review*. Journal of Energy Storage, 2019. **22**: p. 157-175.
32. Naguib, M., et al., *Two-dimensional nanocrystals produced by exfoliation of Ti3AlC2*. Advanced Materials, 2011. **23**(37): p. 4248-4253.
33. Naguib, M., et al., *MXene: a promising transition metal carbide anode for lithium-ion batteries*. Electrochemistry Communications, 2012. **16**(1): p. 61-64.
34. Company, P.C.M.P.L., *Organic phase change material (PLUSICE A70)*. 2011.
35. Ghidiu, M., et al., *Conductive two-dimensional titanium carbide 'clay'with high volumetric capacitance*. Nature, 2014. **516**(7529): p. 78.
36. Hu, T., et al., *Vibrational properties of Ti 3 C 2 and Ti 3 C 2 T 2 (T= O, F, OH) monosheets by first-principles calculations: a comparative study*. Physical Chemistry Chemical Physics, 2015. **17**(15): p. 9997-10003.